

Accepted Manuscript

Magnetic variations in surface soils in the NE Tibetan Plateau indicating the climatic boundary between the Westerly and East Asian summer monsoon regimes in NW China

Jinbo Zan, Xiaomin Fang, Maodu Yan, Weilin Zhang, Zhiguo Zhang

PII: S0921-8181(15)00066-1
DOI: doi: [10.1016/j.gloplacha.2015.03.008](https://doi.org/10.1016/j.gloplacha.2015.03.008)
Reference: GLOBAL 2263

To appear in: *Global and Planetary Change*

Received date: 11 October 2014
Revised date: 21 March 2015
Accepted date: 28 March 2015



Please cite this article as: Zan, Jinbo, Fang, Xiaomin, Yan, Maodu, Zhang, Weilin, Zhang, Zhiguo, Magnetic variations in surface soils in the NE Tibetan Plateau indicating the climatic boundary between the Westerly and East Asian summer monsoon regimes in NW China, *Global and Planetary Change* (2015), doi: [10.1016/j.gloplacha.2015.03.008](https://doi.org/10.1016/j.gloplacha.2015.03.008)

This is a PDF file of an unedited manuscript that has been accepted for publication. As a service to our customers we are providing this early version of the manuscript. The manuscript will undergo copyediting, typesetting, and review of the resulting proof before it is published in its final form. Please note that during the production process errors may be discovered which could affect the content, and all legal disclaimers that apply to the journal pertain.

**Magnetic variations in surface soils in the NE Tibetan Plateau
indicating the climatic boundary between the Westerly and East
Asian summer monsoon regimes in NW China**

Jinbo Zan^a, Xiaomin Fang^a, Maodu Yan^a, Weilin Zhang^a, Zhiguo Zhang^a

^a Key Laboratory of Continental Collision and Plateau Uplift, Institute of Tibetan Plateau Research,
Chinese Academy of Sciences, Beijing 100101, China

Corresponding author. Jinbo Zan, Tel.: +86 10 8409 7172; Fax: +86 10 8409 7079;

E-mail address: zanjb@itpcas.ac.cn

ABSTRACT

Two atmospheric circulation systems, *i.e.*, the mid-latitude Westerlies and the East Asian summer monsoon (EASM), dominate climate change in the NE Tibetan Plateau. However, controversy remains with regard to the climatic boundary between these westerly and monsoon regimes. In this paper, detailed rock magnetic and geochemical Rb/Sr analyses for a larger number of surface soils from a wide area in the NE Tibetan Plateau are presented. They show that surface soils in this region evince relatively significant regional variations in magnetic properties and geochemical characteristics. The magnetic parameters χ_{fd} , χ_{ARM} and geochemical Rb/Sr ratios exhibit higher values in EASM-controlled (humid) areas, and lower values in Westerlies-influenced (arid) areas. These characteristics indicate that such variations in χ_{fd} , χ_{ARM} and Rb/Sr ratios can be regarded as effective indicators of the degree of pedogenesis and weathering in

the NE Tibetan Plateau. Our results also demonstrate that the climatic boundary between the westerly and monsoon regimes approximately overlaps with the boundary of highland meadow and temperate steppe desert/desert in NW China.

Keywords: surface soils; environmental magnetism; Rb/Sr ratio; Tibetan Plateau; climatic boundary

1. Introduction

In the NE Tibetan Plateau (TP), the East Asian winter monsoon does not directly influence the region because of the high elevation of the TP (An et al., 2012). Consequently, two other important atmospheric circulation systems, namely the mid-latitude Westerlies and the East Asian summer monsoon (EASM), dominate climate change in the NE TP (Fig. 1a) (Gao, 1962; Zhao et al., 2007; Chen et al., 2008; An et al., 2012; Li et al., 2012). It has been suggested that the EASM-controlled (humid) and the Westerlies-influenced (arid) areas of Central Asia display distinct meteorological characteristics, but are tied to one another by the exchange of energy, moisture, and momentum of the atmosphere (Gao, 1962; Chen *et al.*, 2008; An *et al.*, 2012). In this context, identification of the climatic boundary between these two regions is essential both to reconstruct the past climates in the NE TP and to understand present climatic conditions. However, due to the region's formidable natural conditions and vast area, meteorological stations have only been established in a few specific areas in the NE TP. A shortage of generic meteorological data has made it difficult to study the climatic boundary between the EASM-controlled (humid) and

Westerlies-influenced (arid) areas of NW China. As a result, many scholars have had to use regional climate models to establish the climatic boundary, though there remains considerable debate over the present limits of EASM influence on the NE TP (Gao, 1962; Zhao et al., 2007; Chen et al., 2008; An et al., 2012; Li et al., 2012) (Fig. 1b).

Fig. 1.

Recently, systematic rock magnetic studies of surface soils from NW China have demonstrated that topmost soils samples from the EASM-controlled (humid) areas and the Westerlies-influenced (arid) areas exhibit distinct magnetic characteristics. In the EASM-controlled (humid) areas, soil weathering and pedogenesis are generally strong, due to abundant precipitation. Variations in the magnetic susceptibility (χ) of surface soils exhibit a strong, positive correlation with mean annual precipitation (MAP), and ultrafine superparamagnetic (SP) and single domain (SD) magnetite/maghemite grains (<100nm) produced during pedogenesis are considered to be mainly responsible for enhancements in χ (Han et al., 1996; Liu et al., 2007; Nie et al., 2010; Song et al., 2014). In contrast, in Westerlies-dominated inland China, westerly air currents from the North Atlantic and the Mediterranean are the chief determinants of moisture content. Due to the high topography of the northern TP, these westerly winds generally release their moisture on the windward side of the mountains, and little westerly moisture penetrates into Westerlies-dominated inland China. This limited precipitation generally yields more weakly-developed soils. Thus, changes in the concentrations of pedogenically-produced SP and SD magnetic

particles do not control the magnetic properties of topmost sediments in these regions. Rather, changes in the concentrations of larger pseudo-single domain (PSD) and multidomain (MD) detrital magnetic minerals derived from source regions appear to be the controlling factors (Zan et al., 2010, 2012, 2015; Xia et al., 2012).

Regional variations in the magnetic properties of surface soils between the EASM-controlled (humid) and the Westerlies-influenced (arid) areas imply that systematic rock magnetic studies of surface soils from the NE TP may provide new information about the climatic boundary between these two regions. In this paper, we present detailed rock magnetic and geochemical Rb/Sr ratio analyses for a larger number of surface soils from a wide area of the NE TP. Our aim is to improve greatly our understanding of the climatic boundary between EASM humid areas and Westerlies-dominated arid areas in NW China.

2. Materials and Methods

A total of 95 surface soil samples were collected from A soil horizons across the NE TP, at elevations between 2000 and 4500m a.s.l. (Fig. 1b). The study area, extending from longitude 90°E to 100° E and latitude 35° N-40° N, covers the Qaidam Basin and the adjacent East Kunlun Mountains, Altyn Mountains and Qilian Mountains (Fig. 1a). The regional climate is characterized by a marked gradient in MAP: from 300-500mm in EASM-controlled (humid) areas, to <50mm in Westerlies-influenced (arid) areas (Gao, 1962). In order to minimize the effect of parent material and geomorphology on the magnetic properties of surface soil samples, all samples

were taken from surface soils developed on eolian loess deposits and on flat geomorphic surfaces. In addition, the samples were taken 5cm from the surface far away from industry and villages to avoid anthropogenic iron contamination.

The samples were air-dried, then were weighed and packed in a nonmagnetic plastic box. Low-frequency and high-frequency magnetic susceptibilities were measured with an AGICO MFK1-FA Kappabridge at frequencies of 976Hz and 15,616Hz, respectively. Mass-specific values (χ) in this paper represent low-frequency measurements. From these data, two measurements of frequency-dependent magnetic susceptibility (χ_{fd} %, defined as $(\chi_{976\text{Hz}} - \chi_{15616\text{Hz}}) / \chi_{976\text{Hz}} \times 100$ %, and χ_{fd} , defined as $\chi_{976\text{Hz}} - \chi_{15616\text{Hz}}$) were then calculated (Forster et al., 1994). Anhysteretic remanent magnetization (ARM) was imparted using a 100mT peak-alternating field with a superimposed 0.05mT direct current bias field. The ARM was normalized by the bias field to obtain ARM susceptibility (χ_{ARM}). Saturation isothermal remanent magnetization (SIRM) was imparted in a 1.5T field using a Magnetic Measurements MPM9 pulse magnetizer, and was measured with a Molspin Minispin magnetometer. A back-field IRM was imparted at 0.3T ($IRM_{-300\text{mT}}$) by reversing the orientation of the samples. The “hard” isothermal remanent magnetization (HIRM) was determined by $(SIRM + IRM_{-300\text{mT}}) / 2$ (Thompson and Oldfield, 1986; Evans and Heller, 2003; Bloemendal and Liu, 2005). Temperature-dependent susceptibility was measured using a MFK1-FA Kappabridge equipped with a CS-4 high-temperature furnace (Agico Ltd., Brno, Czech Republic). High-temperature curves were recorded from room temperature to 700°C; argon atmosphere was used to minimize oxidation. All measurements mentioned above were carried out at the Department of Geosciences of the University of Tübingen.

The Rb and Sr concentrations were determined at Fujian Normal University,

using an ICP-MS (X Series II, Thermo, USA). Replicate analyses of the surface soil samples indicated good reproducibility, *i.e.* analytical uncertainties of <1% (for a more detailed description of the method and sample preparation, see Gallet et al. (1996)). A total of 13 surface soil samples were selected for geochemical Rb/Sr ratio analyses to provide an independent weathering index for comparison with the magnetic susceptibility record.

3. Results

Fig. 2 shows the variations in the magnetic parameters and Rb/Sr ratios for surface soils in the NE TP. The χ varies between 20 and $100 \times 10^{-8} \text{ m}^3/\text{kg}$, with an average of $45 \times 10^{-8} \text{ m}^3/\text{kg}$ (Fig. 2a). Samples 1–26 and 73–87 from the southeast and north of the study area generally have higher χ values than the other samples. For samples 1–26, $\chi_{fd}\%$ varies between 5–11 %, with a mean value of 7.2 % and χ_{fd} generally exceeds $2.5 \times 10^{-8} \text{ m}^3/\text{kg}$ (Figs. 2b-c). The samples 1–13 on the windward sides of the Qinghai Nanshan Mountains and the Qilian Mountains show the highest values of χ_{fd} and $\chi_{fd}\%$. In contrast, χ_{fd} and $\chi_{fd}\%$ for samples 27–95 are generally lower and more constant, with $\chi_{fd}\%$ varying between 2–5% (mean value 3.3%) and χ_{fd} varying between $0.6\text{--}2.1 \times 10^{-8} \text{ m}^3/\text{kg}$ (mean value $1.4 \times 10^{-8} \text{ m}^3/\text{kg}$). All these observations suggest that pedogenically-produced SP magnetic particles abound in samples 1–26.

SIRM is used as an estimate of the total magnetic mineral concentration with grain size larger than the SP/SD threshold (Thompson and Oldfield, 1986; Evans and Heller, 2003). SIRM presents a similar pattern of variation to χ , with high values in

samples 1–26 and 73–87 (Fig. 2d). HIRM values generally range from 1.2×10^{-5} Am²/kg to 4.7×10^{-5} Am²/kg, with an average value of 2.5×10^{-5} Am²/kg (Fig. 2e). χ_{ARM} values vary between 20 and 190×10^{-8} m³/kg (Fig. 2f); they show a similar pattern of variation to the magnetic parameters χ_{fd} , $\chi_{\text{fd}}\%$ and HIRM, and all show higher values in samples 1–26. The Rb/Sr ratios of typical samples from the NE TP range from 0.65 to 1.1 (Fig. 2i).

Fig. 2

The scatterplot indicates that there are strong, positive correlations between χ_{fd} , $\chi_{\text{fd}}\%$ or χ_{ARM} and χ values when samples 73–87 (collected from north of the study area) are excluded (Figs. 3a-c). These characteristics indicate that pedogenically-produced SP and SD magnetic particles play a significant role in accounting for χ variations in these samples. The correlation diagram between χ and χ_{fd} is characterized by a non-zero intercept of the abscissa at $\chi \approx 20 \times 10^{-8}$ m³/kg (Fig. 3a), which reflects the susceptibility value of the parent material. In addition, a strong, positive linear correlation exists between χ_{fd} and χ_{ARM} for all samples (Fig. 3d), which possibly indicates a fixed and consistent grain size distribution of pedogenic magnetite/maghemite (Liu et al., 2004, 2007; Nie et al., 2010). Figs. 3e and f show that there are strong, positive correlations between χ_{fd} or χ_{ARM} and Rb/Sr ratios, suggesting that samples with higher χ_{fd} and χ_{ARM} values have experienced stronger chemical weathering.

Fig. 3

All thermomagnetic curves show a clear Curie temperature at ca. 580°C (Fig. 4a),

indicating that during the experiment newly produced magnetite dominates. Some heating curves demonstrate a significant loss of magnetic susceptibility between 300°C and 400°C (Fig. 4b), suggesting the presence of maghemite. All samples show a clear “hump” in their heating curves at ca. 520°C (Fig. 4a), which can be ascribed either to the Hopkinson effect (Dunlop and Özdemir, 1997) or to the production of magnetite or other higher susceptibility phases during heating (Deng et al., 2001). Because the susceptibility further increases during cooling from 520°C and the cooling curve is irreversible (Fig. 4b), we argue that the Hopkinson effect contributes little to the 520°C susceptibility peak. IRM acquisition curves show that more than 90% of SIRM is acquired below 300mT for most samples (Fig. 4c), suggesting that low-coercivity ferrimagnetic minerals (*i.e.*, magnetite or maghemite) dominate the magnetic properties of the samples. All samples do not become fully saturated even after a field of 1.5T is applied, reflecting the existence of hard magnetic minerals such as goethite and/or hematite.

Fig. 4

4. Discussion

Our rock magnetic results suggest that surface soils in the NE TP show quite significant regional variations in magnetic properties. The most striking feature is that samples 1–26 from the SE of the study area have higher magnetic parameters χ_{fd} , $\chi_{fd}\%$ and χ_{ARM} . Previous work has shown that the parameters χ_{fd} and $\chi_{fd}\%$ are consistent with the degree of pedogenesis and they have thus been regarded as reliable proxies

for the contribution of SP particles during the pedogenic process (Zhou et al., 1990; Evans and Heller, 2003; Liu et al., 2004, 2007; Hao et al., 2008; Song et al., 2014). Compared with χ_{fd} and $\chi_{fd}\%$, the parameter χ_{ARM} is sensitive to grains of $\sim 25\text{--}100\text{nm}$ in size, *i.e.* stable SD and smaller PSD particles (King et al., 1982). At present, there is a consensus that the neoformation of fine-grained magnetite/maghemite particles during pedogenesis in SP and SD grain size regions accounts for the magnetic enhancement found in Chinese paleosols (Zhou et al., 1990; Maher and Thompson 1991; Liu et al., 2004, 2007; Nie et al., 2010). A recent study revealed that SD magnetic particles contributed more than half of the magnetic enhancement in paleosols because they constituted a much higher volume fraction than the SP fraction (Liu et al., 2004). Therefore, higher χ_{fd} , $\chi_{fd}\%$ and χ_{ARM} values for samples 1–26 may indicate that stronger pedogenesis occurred in the SE of the study area, producing higher concentrations of ultrafine SP and SD magnetite/maghemite in the surface soils.

The magnetic parameter ratios χ_{ARM}/SIRM , χ_{ARM}/χ and thermomagnetic plots provide further support for our above inference. The χ_{ARM}/SIRM and χ_{ARM}/χ ratios have been widely accepted as indicators of the grain size of ferrimagnetic minerals, which peak in the SD range and decrease with increasing grain size (Maher, 1988). Compared with χ_{ARM}/χ , χ_{ARM}/SIRM would better reflect the pedogenic SD particles because it is not influenced by the SP fraction. Figs. 2g and h show that the χ_{ARM}/SIRM and χ_{ARM}/χ ratios for samples 1–26 from the SE of the study area are much higher than those from other regions, indicating a higher content of pedogenic SD particles in these samples. The HIRM is generally used as a proxy for the

concentration of the high-coercivity magnetic minerals hematite and goethite, but it is a more sensitive indicator of hematite (Thompson and Oldfield, 1986; King and Channell, 1991; Sangode and Bloemendal, 2004). The lower sensitivity for goethite occurs because goethite does not saturate until the imparted magnetic field is $>4\text{T}$, or even 7T (Sangode and Bloemendal, 2004). Previous studies have found that much pedogenic hematite would be formed as pedogenesis increases, due to strong weathering (Bloemendal and Liu, 2005; Liu et al., 2007; Chen et al., 2010; Liu et al., 2013). Thus, the distinct HIRM peaks in samples 1–26 further indicate that stronger pedogenesis occurred in the SE of the study area as much pedogenic hematite is produced in these samples. In addition, previous temperature-dependent susceptibility (TDS) measurements have suggested that the degree of thermally-induced alteration is closely related to pedogenesis (Deng et al., 2001). Stronger pedogenesis will result in higher maghemite content and a greater susceptibility decrease during thermal treatment (Deng et al., 2001). Our TDS data demonstrate that surface soil samples from the SE of the study area generally display a significant loss of magnetic susceptibility between 300°C and 400°C (Fig. 4a), indicating that stronger pedogenesis has resulted in a higher maghemite content in these samples.

Because Sr resides in the more soluble Na- and Ca-bearing minerals, the removal of these minerals during pedogenesis leads to a relative enhancement of Rb, which resides in the more resistant K-feldspars (Dasch, 1969). Therefore, the variation in Rb/Sr ratios in soil can be regarded as an independent indicator of the degree of pedogenesis (Chen et al., 1999; Liu et al., 2003; Bloemendal and Liu, 2005). The

Rb/Sr and magnetic parameters χ_{fd} or χ_{ARM} for typical surface soil samples from the NE TP are positively correlated (Figs. 4e-f), implying that enhancement of both the Rb/Sr ratio and the magnetic signal in soil were controlled by similar geologic processes, *e.g.* pedogenetic weathering.

All the above observations indicate that changes in the concentrations of pedogenically-produced SP and SD magnetic particles are likely the principal determinants of the magnetic properties of surface soil from the NE TP. However, we note that the pedogenic proxies (*i.e.* χ_{fd} , $\chi_{fd}^{\%}$, χ_{ARM} and the Rb/Sr ratio) for samples 73-87 from the north of the study area are generally lower, while their magnetic concentration parameters χ and SIRM are higher. This discrepancy implies that although all samples are taken from surface soils which have developed on eolian loess deposits, and which are therefore homogeneous in composition, the effects of parent materials on the magnetic properties of these samples cannot be ignored. We argue that coarse, lithogenic, magnetic minerals derived from local sources possibly also contribute to the susceptibility signals of samples 73-87. This seems likely, as, according to the geological map (Qinghai Bureau of Geology and Mineral Resources, 1991), igneous rocks predominate at the NE margin of the TP.

In summary, our rock magnetic and geochemical Rb/Sr ratio analyses indicate that pedogenesis for surface soils in the Westerlies-dominated arid areas is generally weak; stronger pedogenesis occurred in the SE of the study area. A distinct boundary of pedogenic intensity can be observed in the NE TP. Han et al. (1996) examined 63 topsoil samples across the CLP and found that the degree of pedogenesis of surface

soils on the CLP had a strong, positive correlation with MAP. This conclusion is further confirmed by the rock magnetic data of modern soils across the Russian Steppe (Maher et al., 2003) and the CLP (Song et al., 2014). All these investigations indicate a possibly consistent pedogenic model for these very different regions where rainfall controls pedogenic processes. Thus, the strong pedogenesis in the SE of the study area may imply relatively higher precipitation in this area; the clear decrease of magnetically proven pedogenic intensity towards the west indicates the limit of the EASM in NW China. The boundary of highland meadow and temperate steppe desert/desert in the NE TP (Zhao et al., 2007), which can be regarded as an indication of precipitation levels, overlaps approximately with the boundary of pedogenic intensity, providing further support for our above inference. In addition, current meteorological observations demonstrate that MAP reduces significantly from the EASM-controlled (humid) areas (300-500mm) to the Westerlies-influenced (arid) areas (<50mm), which is also consistent with our results. Specifically, for the Tianjun Country in the east of the boundary, the MAP is about 360mm; while in the west, the MAP decreases significantly to 176mm in the Delingha and 45mm in the Golmud, respectively.

However, we also note that a significant difference exists between our results and the results of previous climate model experiments (Chen et al., 2008; Li et al., 2012) (Fig. 1b). We find that surface soil samples 7-13 from the NE slopes of the Qilian Mountains show the highest values of χ_{fd} , $\chi_{fd}\%$, and χ_{ARM} , indicating stronger pedogenesis and higher precipitation on the windward sides of the Qilian Mountains.

These findings imply that EASM moisture extends much farther north along the NE slopes of the Qilian Mountains, something not previously observed by regional climate model experiments.

5. Conclusions

Rock magnetic and geochemical analyses demonstrate that surface soils in the NE TP show quite significant regional variations in magnetic properties and geochemical characteristics. The magnetic parameters χ_{fd} , χ_{ARM} and geochemical Rb/Sr ratios exhibit higher values in the EASM-controlled (humid) areas and lower values in the Westerlies-influenced (arid) areas. These characteristics indicate that variations in χ_{fd} , χ_{ARM} and Rb/Sr ratios can be regarded as effective indicators of the degree of pedogenesis and weathering in the NE TP. Previous work has shown that the degree of pedogenesis of surface soils has a strong, positive correlation with MAP. Thus, the clear decrease of magnetically proven pedogenic intensity towards the west indicates the limit of the EASM in NW China. Our results suggest that the climatic boundary between the westerly and monsoon regimes in NW China overlaps approximately with the boundary of highland meadow and temperate steppe desert/desert in the NE TP. In addition, surface soil samples from the NE slopes of the Qilian Mountains show stronger pedogenesis, implying that EASM moisture extends much farther north along the NE slopes of the Qilian Mountains than previously thought.

Acknowledgement

This work was co-supported by the Strategic Priority Research Program of the Chinese Academy of Sciences (Grant No: XDB03020401), the (973) National Basic Research Program of China (Grant No: 2013CB956400) and the NSFC (Grant Nos: 41321061 and 41102101). All magnetic measurements were carried out at the Department of Geosciences of the University of Tübingen. We thank Drs. Wu Fuli, Wang Shifeng and Hu Kai for their assistance in the field. Special thanks are due to Professor Erwin Appel for his persistent laboratory support. The authors are grateful to Edward Derbyshire for improving the English.

References

- An, Z., Colman, S. M., Zhou, W., Li, X., Brown, E. T., Jull, A. J. T., Cai, Y., Huang, Y., Lu, X., Chang, H., Song, Y., Sun, Y., Xu, H., Liu, W., Jin, Z., Liu, X., Cheng, P., Liu, Y., Ai, L., Li, X., Liu, X., Yan, L., Shi, Z., Wang, X., Wu, F., Qiang, X., Dong, J., Lu, F., Xu, X., 2012. Interplay between the Westerlies and Asian monsoon recorded in Lake Qinghai sediments since 32 ka. *Scientific Reports* 2 (619), 1–6.
- Bloemendal, J. C., Liu, X., 2005. Rock magnetism and geochemistry of two plio-pleistocene Chinese loess-paleosol sequences: Implications for quantitative palaeoprecipitation reconstruction. *Palaeogeography, Palaeoclimatology, Palaeoecology* 226, 149–166, doi: 10.1016/j.palaeo.2005.05.008.
- Chen, T.H., Xu, H.F., Xie, Q.Q., Ji, J.F., Chen, J., Lu, H.Y., Balsam, W., 2010.

- Characteristics and formation mechanism of the pedogenic hematite in Quaternary Chinese loess and paleosols. *Catena* 81, 217–225.
- Chen, F.H., Yu, Z.C., Yang, M.L., Ito, E., Wang, S.M., Madsen, D.B., Huang, X.Z., Zhao, Y., Sato, T., Birks, H.J.B., Boomer, I., Chen, J.H., An, C.B., Wünnemann, B., 2008. Holocene moisture evolution in arid central Asia and its out-of-phase relationship with Asian monsoon history. *Quaternary Science Reviews* 27, 351–364.
- Chen, J., An, Z.S., Head, J., 1999. Variation of Rb/Sr ratios in the loess-paleosol sequences of central China during the last 130,000 years and their implications for monsoon paleoclimatology. *Quaternary Research* 51, 215–219.
- Dasch, E.J., 1969. Strontium isotopes in weathering profiles, deep sea sediments and sedimentary rocks. *Geochim. Cosmochim. Acta* 33, 1521–1552.
- Deng, C. L., Zhu, R. X., Jackson, M. J., Verosub, K. L., Singer, M. J., 2001. Variability of the temperature dependent susceptibility of the Holocene eolian deposits in the Chinese Loess Plateau: A pedogenesis indicator. *Physics and Chemistry of the Earth, Part A* 26, 873–878.
- Dunlop, D. J., Özdemir, Ö., 1997. *Rock Magnetism: Fundamentals and Frontiers*. Cambridge University Press, New York, pp. 1–573.
- Evans, M. E., Heller, F., 2003. *Environmental Magnetism: Principles and Applications of Enviromagnetics*. *International Geophysics* 86, Academic, Amsterdam.
- Forster, T., Evans, M. E., Heller, F., 1994. The frequency dependence of low field

- susceptibility in loess sediments. *Geophysical Journal International* 118(3), 636–642.
- Gallet, S., John, B. M., Toril, M., 1996. Geochemical characterization of the Luochuan loess–paleosol sequence, China, and paleoclimatic implications. *Chemical Geology* 133, 67–88.
- Gao, Y.X., 1962. On some problems of Asian monsoon. In: Gao, Y.X. (Ed.), *Some Questions about the East Asian Monsoon*. Chinese Science Press, Beijing, pp. 1–49 (in Chinese).
- Han, J., Lu, H., Wu, N., Guo, Z., 1996. The magnetic susceptibility of modern soils in china and climate conditions. *Studia Geophysica et Geodetica* 40, 262–275.
- Hao, Q., Oldfield, F., Bloemendal, J., Guo, Z., 2008. Particle size separation and evidence for pedogenesis in samples from the Chinese Loess Plateau spanning the last 22 Ma. *Geology* 36 (9), 727–730
- King, J., Banerjee, S. K., Marvin, J., Özdemir, Ö., 1982. A comparison of different magnetic methods for determining the relative grain size of magnetite in natural materials: Some results from lake sediments. *Earth and Planetary Science Letters* 59, 404–419.
- King, J., Channell, J., 1991. Sedimentary magnetism, environmental magnetism, and magnetostratigraphy. *Review of Geophysics* 39, 358–370.
- Li, Y., Wang, N. A., Chen, H., Li, Z., Zhou, X., Zhang, C., 2012. Tracking millennial-scale climate change by analysis of the modern summer precipitation in the marginal regions of the Asian monsoon. *Journal of Asian Earth Sciences* 58, 78–

87.

- Liu, X. M., Rolph, T., An, Z. S., Hesse, P., 2003. Paleoclimatic significance of magnetic properties on the Red Clay underlying the loess and paleosols in China. *Palaeogeography, Palaeoclimatology, Palaeoecology* 199, 153-166.
- Liu, Q. S., Banerjee, S. K., Jackson, M. J., Maher, B. A., Pan, Y. X., Zhu, R. X., Deng, C. L., Chen, F. H., 2004. Grain sizes of susceptibility and anhysteretic remanent magnetization carriers in Chinese loess/paleosol sequences. *Journal of Geophysical Research* 109, B03101, doi:10.1029/2003JB002747.
- Liu, Q., Deng, C., Torrent, J., Zhu, R.X., 2007. Review of recent development in mineral magnetism of the Chinese loess. *Quaternary Science Reviews* 26, 368–385.
- Liu, Z.F., Liu, Q.S., Torrent, J., Barron, V., Hu, P.X., 2013. Testing the magnetic proxy χ_{FD}/HIRM for quantifying paleoprecipitation in modern soil profiles from Shaanxi Province, China. *Global Planet Change* 110, 368-378.
- Maher, B. A., 1988. Magnetic properties of some synthetic sub-micron magnetites. *Geophysical Journal* 94, 83–96.
- Maher, B. A., Taylor, R. M., 1991. Mineral magnetic record of the Chinese loess and paleosols. *Geology*, 19, 3–6.
- Maher, B. A., Alekseev, A., Alekseeva, T., 2003. Magnetic mineralogy of soils across the Russian Steppe: climatic dependence of pedogenic magnetite formation. *Palaeogeography, Palaeoclimatology, Palaeoecology* 201, 321–341.
- Nie, J. S., Song, Y. G., King, J. W., Egli, R., 2010. Consistent grain size distribution

- of pedogenic maghemite of surface soils and Miocene loessic soils on the Chinese Loess Plateau. *Journal of Quaternary Science* 25(3), 261–266.
- Qinghai Bureau of Geology and Mineral Resources, 1991. *Regional Geology of Qinghai Province*. Geological Publishing House, Beijing, pp. 662 (in Chinese with English brief introduce).
- Sangode, S. J., Bloemendal, J. C., 2004. Pedogenic transformation of magnetic minerals in Pliocene–Pleistocene palaeosols of the Siwalik Group, NW Himalaya, India. *Palaeogeography, Palaeoclimatology, Palaeoecology* 212, 95–118.
- Song, Y., Hao, Q. Z., Ge, J. Y., Zhao, D. A., Zhang, Y., Li, Q., Zuo, X. X., Lü, Y. W., Wang, P., 2014. Quantitative relationships between magnetic enhancement of modern soils and climatic variables over the Chinese Loess Plateau. *Quaternary International* 334–335, 119–131.
- Thompson, R., Oldfield, F., 1986. *Environmental Magnetism*, Allen and Unwin, Winchester, Mass., doi:10.1007/978-94-011-8036-8.
- Xia, D. S., Jia, J., Wei, H.T., Liu, X. B., Ma, J. Y., Wang, X. M., Chen, F.H., 2012. Magnetic properties of surface soils in the Chinese Loess Plateau and the adjacent Gobi areas, and their implication for climatic studies. *Journal of Arid Environments* 78, 73–79.
- Zan, J. B., Fang, X. M., Nie, J. S., Yang, S. L., Song, C. H., Dai, S. , 2010. Magnetic properties of surface soils across the southern Tarim Basin and their relationship with climate and source materials. *Chinese Science Bulletin* 55, 1–7, doi: 10.1007/s11434-010-0000-2.

- Zan, J. B., Fang, X. M., Nie, J. S., Teng, X. H., Yang, S. L., 2012. Rock magnetism in loess from the middle Tian Shan: Implications for paleoenvironmental interpretations of magnetic properties of loess deposits in Central Asia. *Geochemistry, Geophysics, Geosystems* 13, Q10Z50, doi:10.1029/2012GC004251.
- Zan, J. B., Fang, X. M., Yang, S. L., Yan, M.D., 2015. Bulk particle size distribution and magnetic properties of particle-sized fractions from loess and paleosol samples in Central Asia. *Geochemistry, Geophysics, Geosystems* 16, doi:10.1002/2014GC005616.
- Zhao, Y., Yu, Z.C., Chen, F.H., Ito, E., Zhao, C., 2007. Holocene vegetation and climate history at Hurleg Lake in the Qaidam Basin, northwest China. *Review of Palaeobotany and Palynology* 145, 275–288.
- Zhou, L. P., Oldfield, F., Wintle, A. G., Robinson, S. G., Wang, T. J., 1990. Partly pedogenic origin of magnetic variations in Chinese loess. *Nature* 346, 737–739.

Figure captions

Fig. 1. (a) Satellite image and geographic map showing the location of the study area within the Asian arid inland and East Asian monsoon-moistened regions. (b) Digital elevation map of the NE TP showing sampling locations. Red solid circles show the locations of surface soil samples. The black line shows the present limit of the EASM in NW China (Chen et al., 2008). The white line approximately represents the boundary of highland meadow and temperate steppe desert/desert (Zhao et al., 2007), which is regarded as an indication of precipitation levels. The narrow arrows indicate the main wind directions observed in the Qaidam Basin.

Fig. 2. Variations in magnetic parameters and Rb/Sr ratios of surface soil samples in the NE TP. The horizontal dashed line indicates the clear decrease of magnetically proven pedogenic intensity towards the west. The two areas highlighted in yellow indicate that coarse, lithogenic, magnetic minerals derived from local sources possibly also contribute to the susceptibility and SIRM signals of samples 73-87.

Fig. 3. The relations between: (a) χ_{fd} versus χ ; (b) $\chi_{fd}\%$ versus χ ; (c) χ_{ARM} versus χ ; (d) χ_{ARM} versus χ_{fd} ; (e) χ_{fd} versus Rb/Sr ratio; and (f) χ_{ARM} versus Rb/Sr ratio for surface soil samples from the NE TP. Note the positive correlations between χ_{fd} , $\chi_{fd}\%$ or χ_{ARM} and χ in Figs. a-c when surface samples 73-87 collected from the north of the study area are excluded.

Fig. 4. High-temperature magnetic susceptibility curves (κ -T curves) (a–b) and isothermal remanent magnetization (IRM) acquisition curves (c) of typical surface soil samples from the NE TP. Samples in Fig. b were heated to 520°C; dashed lines indicate cooling curves.

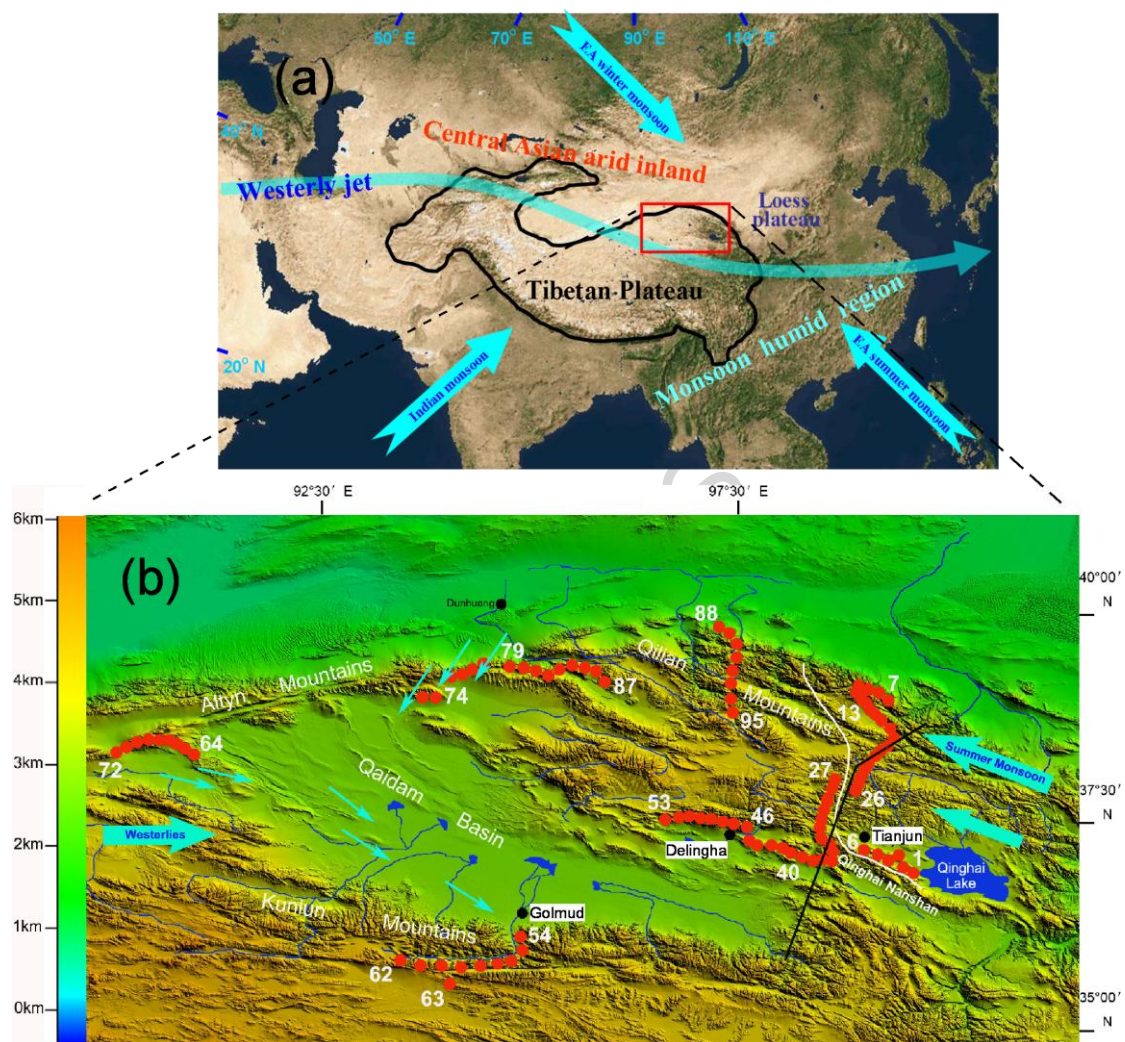


Figure 1

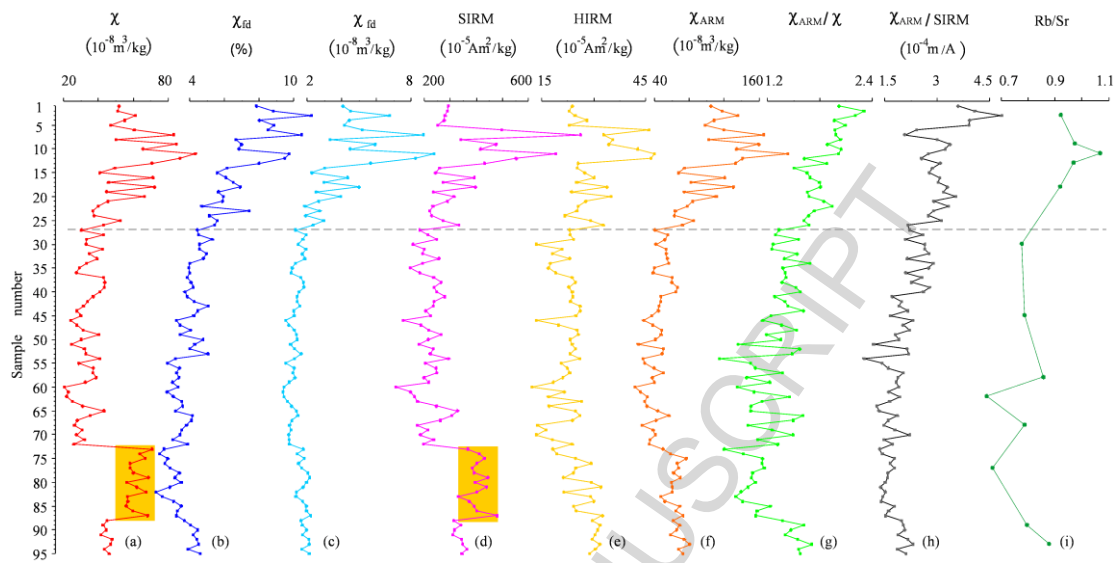


Figure 2

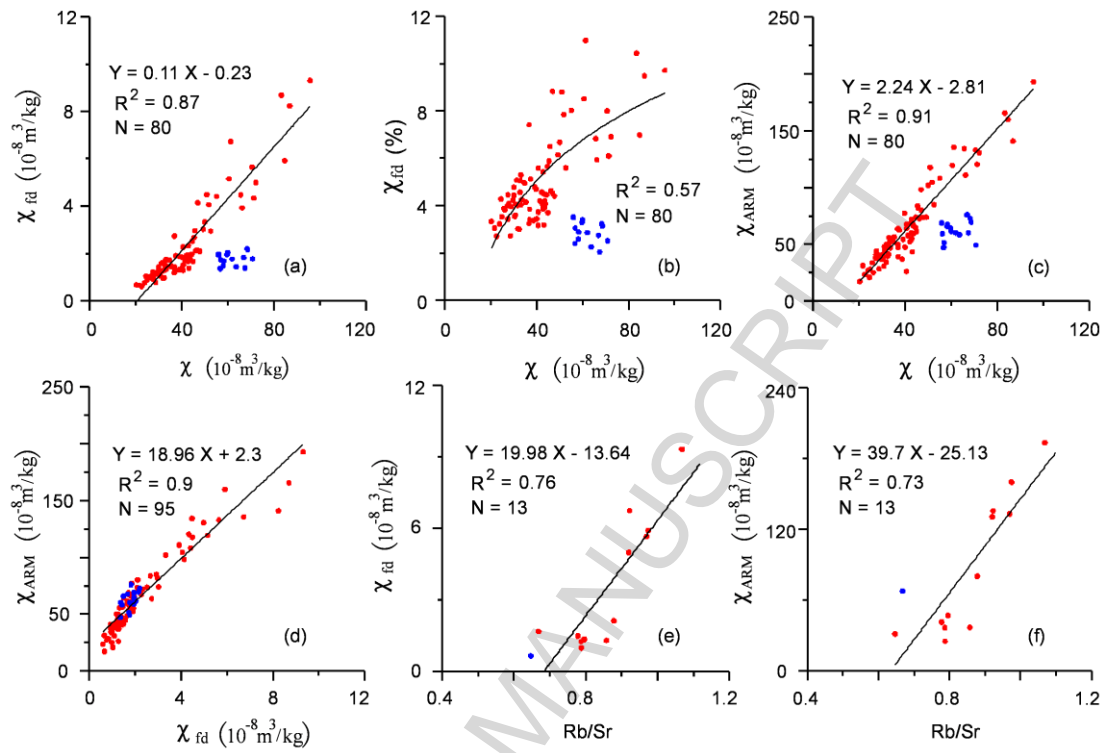


Figure 3

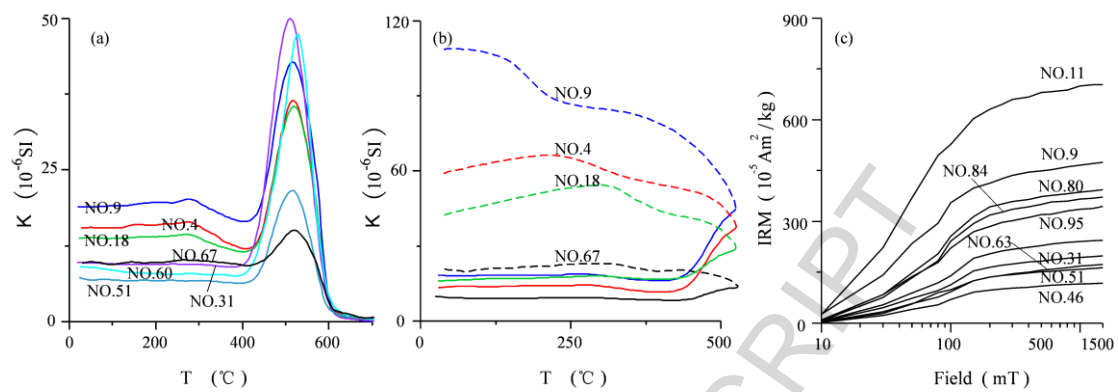


Figure 4

Highlights

Magnetic properties of surface soils in the NE Tibetan Plateau were studied;

Pedogenesis controls the magnetic variations of surface soils;

The decrease of pedogenic intensity towards the west indicates the limit of the EASM

ACCEPTED MANUSCRIPT